

A New Synthetic Route to Wüstite

Jung-Chul Park,* Don Kim,[†] Choong-Sub Lee,[‡] and Dong-Kuk Kim[§]

Department of Chemistry, Silla University, Pusan 617-736, Korea

[†]*Department of Chemistry, Pukyong National University, Pusan 608-737, Korea*

[‡]*Department of Physics, Pukyong National University, Pusan 608-737, Korea*

[§]*Department of Chemistry, Kyungpook National University, Taegu 702-701, Korea*

Received December 28, 1998

Wüstite with NaCl structure is successfully synthesized in a quartz tube sealed under vacuum ($\approx 1 \times 10^{-3}$ torr). Hematite in an evacuated quartz tube progressively loses oxide ion at 1373 K. XRD patterns disclose that α -Fe₂O₃ is transformed into the Fe₃O₄ after heat treatment at 1373 K for 32 h, and the poorly crystallized FeO is appeared after heat treatment for 48 h. Finally, α -Fe₂O₃ is completely transformed into the well crystallized Fe_{0.935}O after heat treatment for 84 h. The electrical resistivity, ac-susceptibility measurement, Mössbauer spectroscopy, and x-ray absorption spectroscopy corroborate the structural phase transition on the iron oxides prepared in a sealed quartz tube depending on the heating time at 1373 K.

Introduction

Unlike other transition metal oxides, the stoichiometric iron monoxide cannot exist as a stable phase, so the nonstoichiometric iron monoxide, wüstite has been extensively studied as the model of a nonstoichiometric phase. A stable, cation-deficient phase, Fe_{1-x}O ($0.83 < x < 0.95$) exists at 0.1 MPa pressure and temperatures higher than 840 K.¹ This phase decomposes to Fe metal and Fe₃O₄ when cooled slowly to temperatures lower than 840 K. If, however, the Fe_{1-x}O is rapidly quenched from the equilibrium region, this phase can be obtained as a metastable one at room temperature.²

The nonstoichiometry of wüstite varies with the oxidation of divalent iron to trivalent iron as a function of temperature (T) and oxygen partial pressure (P_{O₂}). In comparison with other transition metal oxides, such as Ni_{1-x}O, Co_{1-x}O, or Mn_{1-x}O with very small x ($x < 10^{-4}$) at low oxygen partial pressure, wüstite exhibits a minimal cation deficit of about 5%.³

The nonstoichiometric wüstites are prepared from the mixtures of iron(III) oxide and iron metal powder. The mixtures of Fe and Fe₂O₃ with overall Fe/O ratio in the range 0.88- 0.95 are heated in evacuated and sealed vitreous silica tubes at 1273 K for 2 days and quenched down to room temperature.^{4,5} It should be mentioned that the preparation route is composed of two steps including the reduction step under dry hydrogen gas at 1120 K from the Fe₂O₃ to the pure metallic iron. And also, this method is too much troublesome since it is very difficult to control Fe/O ratio due to the high reactivity of Fe metal powder. Thus, in this study, we will try to synthesize directly wüstite, Fe_{1-x}O from the Fe₂O₃ using one step reaction.

It is also motivated that the reduction of ferric oxide has been extensively studied for its importance to iron making and steel making.⁶⁻⁸ The kinetics of reduction of Fe₂O₃ has been frequently studied by measuring the weight loss⁹⁻¹¹ and electrical conductivity of ferric oxides¹²⁻¹⁴ during reduction.

The extent of the reduction was found to depend on the gas composition, reduction temperature, and pellet thickness. Furthermore, the surface reaction was occurred during the low temperature reduction of sintered hematite pellets under hydrogen between 573 and 773 K, and the reactivity of hematite toward reduction under hydrogen was determined by the value of δ (in the formula Fe₂O_{3- δ}).¹⁵ It should be pointed out that the well-defined reduction products of Fe₂O₃ can be obtained under optimal conditions of temperature and oxygen partial pressure. More precisely, the Fe₂O₃ can lose lattice oxide ions (O²⁻) at high temperature under a mild reduction atmosphere, such as vacuum. As more oxygen vacancies are generated, the hematite deviates from stoichiometry, that is, may be transformed into magnetite or wüstite.

Based on these facts above mentioned, we try to synthesize directly wüstite from the Fe₂O₃ using vacuum ($\approx 1 \times 10^{-3}$ torr).

Experimental Section

The FeO used in this investigation was prepared from iron(III) oxide. The α -Fe₂O₃ (Aldrich, 99.998%, and $w \approx 150$ mg for each pellet) was pelletized and put into the quartz tube, then the quartz tube was sealed under vacuum ($\approx 1 \times 10^{-3}$ torr). The Fe₂O₃ pellets in the sealed quartz tubes were heated in an electric furnace at 1373 K as a function of time, and cooled down to room temperature in an electric furnace.

Powder X-ray diffraction data were obtained with Rigaku D-max 2400 using Cu K α radiation.

The resistivities of samples were measured by four probe dc method using a nanovoltmeter (Keithley 182) and a current source (Keithley 224). Temperature of the sample was controlled by a closed cycle helium refrigerator (APD HC-2) and a temperature controller (Lake Shore M330).

Ac-susceptibility measurement was performed by an ac-susceptometer (Lake Shore 7130) with 2×10^{-8} emu/g sensi-

tivity.

The Mössbauer spectroscopy studies were carried out at 298 K with ^{57}Co source doped in metallic rhodium which was oscillated in a sinusoidal mode. The doppler velocity of spectra was calibrated with iron metal foil (25 μm in thickness).

X-ray absorption near edge structure (XANES) spectra were measured at the beam line 3C1 of the Pohang Accelerator Laboratory, operated at 2.0 GeV with the stored current of ca. 100-150 mA. Samples were ground to fine powder in a mortar, and then spread uniformly onto an adhesive tape, which was folded into some layers to obtain an optimum absorption jump. All the data were recorded in a transmission mode at room temperature using the double crystal Si(111) monochromator, which was detuned and stabilized to 60% of the incident intensity, I_0 , at the absorption edge in order to reject higher harmonics. The energy was calibrated to the edge position, 7112 eV, of a simultaneously measured Fe metal. Ionization chambers filled with N_2 were used as detection scheme for photon intensities.

Results and Discussion

Figure 1-a) reveals that $\alpha\text{-Fe}_2\text{O}_3$ is transformed into the Fe_3O_4 after treatment at 1373 K for 32 h. After thermal treatment at 1373 K for 48 h, the structural variation of $\alpha\text{-Fe}_2\text{O}_3$ is shown in Figure 1-b). It might be assured that this XRD pattern is very similar to that of Fe_{1-x}O . After thermal treatment at 1373 K for 84 h, the well crystallized Fe_{1-x}O is formed as shown in Figure 1-c). Based on the value of unit cell parameters of Fe_{1-x}O ($a = 4.303 \text{ \AA}$) estimated from XRD pattern in Figure 1-c), the composition x is determined to 0.935 according to the linear relation, $a = 4.334 - 0.478 x$.¹⁶

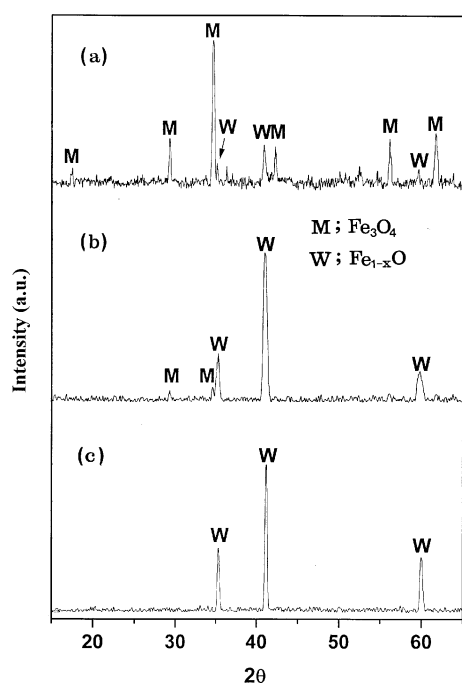
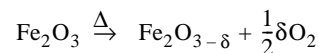


Figure 1. XRD patterns of iron oxides prepared under vacuum.

As the heating time is prolonged, the remaining hematite deviates from stoichiometry. So, this reaction can be expressed, as follows;



where δ refers to the extent of oxygen vacancy.

From the XRD patterns of thermally treated Fe_2O_3 , it can be deduced that the structural evolution from $\alpha\text{-Fe}_2\text{O}_3$ (hematite, corundum structure) to $\text{Fe}_{0.935}\text{O}$ (wüstite, NaCl structure) is due to the removal of an oxide ion O^{2-} from $\alpha\text{-Fe}_2\text{O}_3$ lattice. It should be pointed out that vacuum ($\approx 1 \times 10^{-3}$ torr) would play an important role for the deintercalation of oxide ion from Fe_2O_3 lattice. The well crystallized $\text{Fe}_{0.935}\text{O}$ was annealed at 520 K for 7 days. XRD analysis revealed that wüstite decomposes to the two phase mixture of iron and magnetite, which is in agreement with the disproportionation reaction of wüstite reported.¹⁷

The electrical resistivity as a function of temperature corroborates the structural evolution of iron oxides as prepared. As shown in Figure 2, the electrical resistivity of $\text{Fe}_{0.935}\text{O}$ has the higher value than that of magnetite. The electrical resistivity of single crystal magnetite has a good coincidence with that of reported literature.¹⁸⁻²⁰ The electronic structure of wüstite can be described in terms of molecular orbital diagram of FeO_6^{10-} for Fe^{2+} in octahedral coordination. The energy levels for FeO_6^{10-} cluster is determined by overlapping between Fe 3d orbitals and O 2p orbitals, which finally forms into the bands. Wüstite is classified as the p-type semiconductor with the band gap of 2.3 eV.¹⁹ The band gap of Fe_3O_4 is small (0.1 eV), so magnetite shows the lowest resistance of any iron oxide. In edge-sharing octahedra, the Fe^{2+} and Fe^{3+} ions on the octahedral sites are close together, and in consequence the charge carriers easily exchange between the Fe^{2+} and Fe^{3+} in octahedral sites, which results in the lowest resistivity.

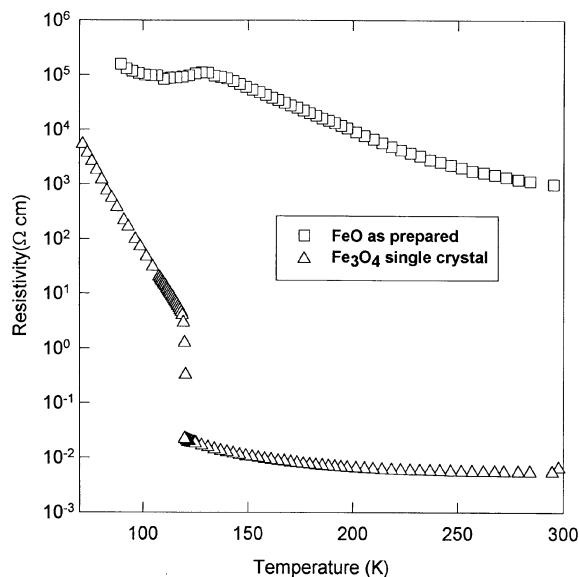


Figure 2. Electrical resistivity of iron oxides prepared under vacuum.

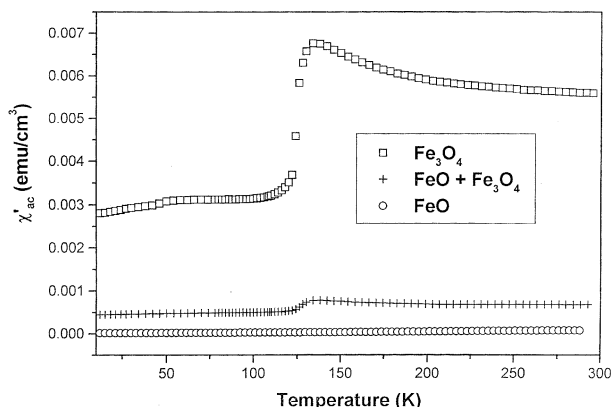


Figure 3. Susceptibility as a function of temperature for iron oxides.

According to the previous results,^{21,22} ac-susceptibility measurement is a very useful noncontact method to confirm small deviation of nonstoichiometry in magnetite from the measured Verwey transition temperature. We expected that if some parts of a sample is close to ideal magnetite, ac-susceptibility changes in sudden at the corresponding temperature of the nonstoichiometry of the magnetite phase. In Figure 3, there is an abrupt susceptibility change for Fe_3O_4 sample around 120 K, and the change is considerably reduced for Fe_{1-x}O and Fe_3O_4 mixture. More especially, there is no change for $\text{Fe}_{0.935}\text{O}$ sample. It should be mentioned that the change is very closely related with Verwey transition of magnetite as discussed.^{21,22} So, it is found that the fraction of Fe_3O_4 obtained after heating Fe_2O_3 for 32 h is very close to the ideal magnetite. But the fraction of magnetite in Fe_{1-x}O and Fe_3O_4 mixture might be much lower than that of Fe_3O_4 (top in the curve) as the jump height in the plot depends on the fraction of magnetite phase. Clearly, $\text{Fe}_{0.935}\text{O}$ sample is an ideal magnetite free one as confirmed by XRD analysis.

The Mössbauer spectra of $\alpha\text{-Fe}_2\text{O}_3$ heated at 1373 K as a function of time are shown in Figure 4. For $\alpha\text{-Fe}_2\text{O}_3$ (99.998%, Aldrich), this spectrum yields $\delta = 0.42 \text{ mmS}^{-1}$, $H_{\text{eff}} = 524 \text{ kOe}$, and the effective quadrupole splitting is -0.10 mmS^{-1} .²⁰ After thermal treatment of $\alpha\text{-Fe}_2\text{O}_3$ at 1373 K for 32 h, the Mössbauer spectrum (b) exhibits hyperfine magnetic splitting. This spectrum consists of two sextets which are attributed to tetrahedral sites (A site; Fe^{3+}) and octahedral sites (B sites; Fe^{3+}). This is in accordance with the well known Mössbauer spectrum of Fe_3O_4 .²³ However, the notable thing is found in the vicinity of $v = 1 \text{ mmS}^{-1}$, which results from the minor portion of Fe_{1-x}O with isomer shift of doublet $\delta = 0.98 \text{ mmS}^{-1}$ (relative to iron metal). From the area of peak corresponding to each compound, the relative content (%) of Fe_3O_4 and Fe_{1-x}O was determined as 82% and 12%, respectively. After thermal treatment at 1373 K for 48 h, the intensities of two sextets attributed to Fe_3O_4 were decreased on a large scale, but there still are some traces of two sextets (as the mark of arrow). Based on the area ratio of the peak, the relative content (%) of Fe_3O_4 and Fe_{1-x}O could be determined as 18% and 82%, respectively. The Möss-

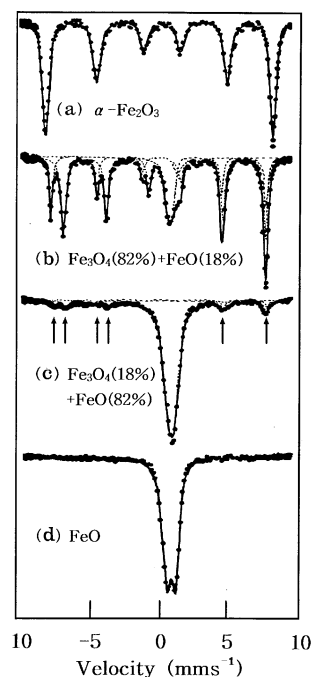


Figure 4. Mössbauer spectra of iron oxides.

bauer spectrum of $\alpha\text{-Fe}_2\text{O}_3$ after thermal treatment at 1373 K for 84 h was obtained as shown in Figure 4-d). The spectrum corresponds to the well crystallized $\text{Fe}_{0.935}\text{O}$ with isomer shift $\delta = 0.98$ and quadrupole splitting $\Delta = eqQ/2 = 0.66$. For the well crystallized $\text{Fe}_{0.935}\text{O}$, the central part of the spectrum exhibits only a slightly separated doublet. As expected for a compound with cubic structure, it is presumed that the Mössbauer spectrum of stoichiometric iron monoxide consists of a single line at room temperature. The spectrum of the nonstoichiometric compound consists of an asymmetrically formed doublet with contribution from Fe^{3+} resonance and from two quadrupole split Fe^{2+} in the structure (*i.e.* the variation in Fe content and vacancy level).

Since detailed information on the valence and local environments of the specific element can be obtained from the x-ray absorption near edge structure (XANES), the evolution of the Fe K-edge XANES spectra for iron oxides according to the reaction time is depicted in Figure 5. For comparison, the figure also includes the Fe K-edge XANES for the ground sample (b) of single crystal Fe_3O_4 and Fe metal foil (f). With increasing reaction time, the overall near edge structure shifts to lower energies. However, the two samples heated for more than 48 h shows almost the same absorption edge feature. For more detail comparison of XANES spectral features, their second derivatives are shown in lower panel of Figure 5. In the second-derivative spectra, we can see that (b) and (c) spectra are similar, and also (d) and (e) spectra are similar. In the upper part of Figure 5, the similarity of (d) and (e) spectra was already shown, but (b) spectrum is seen to be different from (c) one. Here, it should be noted that more the exact electronic and local structural information can be deduced when XANES spectra are compared in their derivatives. Turning to the comparison of the

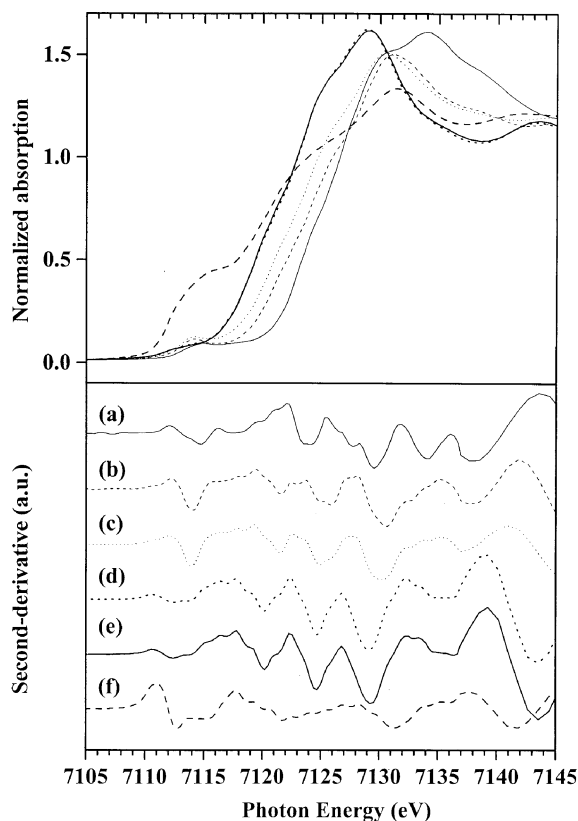


Figure 5. XANES spectra (upper panel) at Fe K-edge and their second derivatives (lower panel) of α -Fe₂O₃ (a), Fe₃O₄ (b), the sample after heating α -Fe₂O₃ at 1373 K for 32 h (c), 48 h (d), 84 h (e), and the reference Fe metal (f).

second-derivative spectra for iron oxides again, the peak appearing around 7112–7114 eV, which is assigned to $1s \rightarrow 3d$ transition with dipole and quadrupole components,²⁴ shows small doublet feature for (a), (d), and (e), but large single feature for (b) and (c). This spectral difference is due to the electronic structural difference induced from the change of local structure around iron ion. The intensity of this peak is well known to increase when the symmetry of the iron site is lowered.²⁵ And also, the doublet feature in (a), (d), and (e) spectra means that the antibonding d -bands consisting of conduction band are doubly split above Fermi level, whereas the singlet feature in (b) and (c) spectra means the antibonding d -bands above Fermi level to be overlapped. In special, the energy difference of doublet feature for (e), 1.5 eV, is in good agreement with the calculated one²⁶ for FeO. In addition, the relative intensity of lower and higher energy features in a doublet is also in good agreement with the previously reported Fe L_{II,III}-edge XANES spectra²⁷ for the α -Fe₂O₃ and Fe_{1-x}O. From these facts, it is thought that the samples evacuated more than 48 h at 1373 K consist of basically wüstite, Fe_{1-x}O. Careful inspection of the (b) and (c) spectra reveals that they are slightly different from each other in the higher energy region above 7120 eV, which indicates in a simple sense that (c) sample can be a mixed form of α -Fe₂O₃ and Fe₃O₄, or Fe₃O₄ and Fe_{1-x}O. Therefore we have compared the average spectra of $(1-x)(a) + x(b)$ or $(1-$

$x)(b) + x(e)$ with (c) spectrum, and consequently the average spectrum of $0.8(b) + 0.2(e)$ was well fitted to (c) spectrum. This result is well consistent with the fact that the sample evacuated for 32 h at 1373 K consist of a mixed form of 82% Fe₃O₄ and 18% FeO by means of the Mössbauer spectra. However, as stated above, there is no considerable difference between (d) and (e) spectra, which might be due to the intrinsic resolution of x-ray absorption spectroscopy in case of the samples evacuated for more than 48 h at 1373 K.

Conclusion

Iron(II) oxide with NaCl structure is successfully synthesized in a sealed quartz tube under vacuum. Hematite in an evacuated quartz tube progressively loses oxide ion at 1373 K depending on the heating time. XRD patterns disclose that α -Fe₂O₃ transforms into the Fe₃O₄ after heat treatment at 1373 K for 32 h, and the poorly crystallized Fe_{1-x}O is appeared after heat treatment for 48 h. Finally, α -Fe₂O₃ is completely transformed into the well crystallized Fe_{0.935}O after heat treatment for 84 h.

The electrical resistivity, ac-susceptibility measurement, Mössbauer spectroscopy, and x-ray absorption spectroscopy corroborate the structural phase transition on the iron oxides prepared in a sealed quartz tube. Moreover, the newly prepared Fe_{0.935}O was considerably stable at room temperature even in a strong basic solution (1 N KOH) under a polarizing potential.

It is assured that vacuum treatment play an important role to remove oxide ion from α -Fe₂O₃ lattice, or in other words, it can be regarded as a mild reduction atmosphere.

Therefore, it is concluded that the new preparation route using vacuum technique promises well the nonstoichiometric wüstite, Fe_{0.935}O.

Acknowledgment. This work was supported by the Korean Ministry of Education through the research Fund (BSRI-96-2455).

References

1. Darkin, L. S.; Gurry, R. W. *J. Am. Chem. Soc.* **1945**, *47*, 2876.
2. Hentschel, B. Z. *Naturforschung* **1970**, *25*, 1996.
3. Schweika, W.; Hoser, A.; Martin, M.; Carlsson, A. E. *Phys. Rev. B*, **1995**, *51*, 15771.
4. Stolen, S.; Glöckner, R.; Gronvold, F.; Atake, T.; Izumisawa, S. *American Mineralogist* **1996**, *81*, 973.
5. Fjellvag, H.; Gronvold, F.; Stolen, S. *J. Solid State Chem.* **1996**, *124*, 52.
6. Coulombo, V.; Gazzarini, F.; Lanzaveccia, G. *Mater. Sci. Eng.* **1967**, *2*, 117.
7. Wimmers, O. J.; Arnoldy, P.; Monjilin, J. A. *J. Phys. Chem.* **1986**, *90*, 1331.
8. Gleitzer, C. *Solid State Ionics* **1990**, *38*, 133.
9. Shimokawabe, M.; Furuichi, R.; Ishii, T. *Thermochim. Acta* **1979**, *28*, 287.
10. Hutchings, K. M.; Smith, J. D.; Yoruk, S.; Hawkins, R. J. *Ironmaking Steelmaking* **1987**, *14*, 103.

11. Chinje, U. F.; Jeffes, J. H. E. *Ironmaking Steelmaking* **1990**, *17*, 317.
 12. Kim, K. H.; Choi, J. S. *J. Phys. Chem.* **1981**, *85*, 2447.
 13. Vasiliev, A. A.; Polykarpov, M. A. *Sensors and Actuators* **1992**, *B7*, 626.
 14. Khader, M. M.; Anadouli, B. E. EL.; EL-Naggar, E.; Ateya, B. G. *J. Solid State Chem.* **1991**, *93*, 283.
 15. Abd Elhamid, M. H.; Khader, M. M.; Mahgoub, A. E.; Anadouli, B. E. EL.; Ateya, B. G. *J. Solid State Chem.* **1996**, *123*, 249.
 16. Mc Cammon, C. A.; Liu, L. *Phys. Chem. Miner.* **1984**, *10*, 106.
 17. Andersson, B.; Sletnes, J. O. *Acta Crystallogr.* **1977**, *Sect. A*, *A33*, 268.
 18. Mollomg, J. J. *Alloy and Compounds* **1995**, 229, 24.
 19. Honig, J. M. *Proc. Indian Acad. Sci.(Chem. Sci.)* **1986**, *96*, 391.
 20. Kozlowski, A.; Metcalf, P.; Kakol, Z.; Honig, J. M. *Phys. Rev. B* **1996**, *53*(22), 15113.
 21. Kim, D.; Lee, C. S.; Kim, Y. I. *Bull. Korean Chem. Soc.* **1998**, *19*, 533.
 22. Aragon, R.; Buttery, D. J.; Shepherd, J. P.; Honig, J. M. *Phys. Rev. B* **1985**, *31*, 430.
 23. Bearden, J. A.; Burr, A. F. *Rev. Mod. Phys.* **1989**, *39*, 125.
 24. Sasaki, S. *Rev. Sci. Instrum.* **1995**, *66*, 1573.
 25. Loeb, K. E.; Zaleski, J. M.; Westre, T. E.; Guajardo, R. J.; Mascharak, P. K.; Hedman, B.; Hodgson, K. O.; Solomon, E. I. *J. Am. Chem. Soc.* **1995**, *117*, 4545.
 26. Hugel, J.; Kamal, M. *Solid State Commun.* **1996**, *100*, 457.
 27. Gautier-Soyer, M. *J. Europ. Ceram. Soc.* **1998**, *18*, 2253.
-